A review of multiple dark matter signatures: indirect searches and machine learning.

Viviana Gammaldi, Jaume Zuriaga-Puig

December 29, 2022

Abstract

What is Dark Matter (DM) and how it manifests besides the gravitational evidences? This is one of the most intriguing open question in cosmology and particle physics so far. In this invited contribution to the 2021 edition of the Vulcano Workshop, we briefly review the indirect searches for multiple DM signatures in astrophysical targets. We review the multi-messenger and multi-wavelength approach to the indirect detection of Weakly Interacting Massive Particles (WIMPs), with a particular focus on the log-parabola data-driven approach for ML application.

1 Introduction

For more than 50 years now, Dark Matter (DM) has been escaped researchers all around the world. DM represents more than 27% of the total content of the universe, yet no one has managed to find any trace of its existence beyond the well-known gravitational effects. One of the main problems is that we do not know what it is made of. Many candidates have been proposed during the years (see e.g. [1, 2]). Among other candidates, Weakly Interacting Massive Particles (WIMPs) represent an elegant way of explaining the existence of the cold DM (CDM) component of the Universe, by considering that any unknown elementary particle must exist beyond the Standard Model (SM) of particle physics. The CDM WIMP candidates would allow to solve open questions in both SM physics and cosmology [3]. The existence of such WIMPs may be proved through different types of experiments. A trace of the scattering of light WIMPs with atoms of the SM, is expected in direct searches with underground laboratories [4]. A missing energy is expected in the products of the collision e.g. of two protons in particle accelerators, as a signature of DM particle of masses up to a few TeV [5]. Among other WIMP candidates, the supersymmetric (SUSY) models benefits of strong approval for years. Nonetheless, null result of the Large Hadron Collider (LHC) below the TeV energy scale has - at least -

weakened the popularity of that models. Many other theoretical models could justify the existence of DM candidates at the TeV scale (see e.g. Brane world DM [6], Feebly Interacting Massive Particle [7] and superWIMP [8]). Indirect detection allows to search for WIMP candidates of a broad range of energy up to hundrends of TeV, by studying the flux of astrophysical targets [9]. Although, not all the DM candidates have an expected signature in the framework of indirect detection.

In these proceedings we focus on multiple signatures of WIMP candidates. In Section 2, we review the fundamental equations for both the multi-messenger and multi-wavelength approach to WIMP searches. In Section 3, we discuss a data-driven approach adopted to introduce the WIMP candidate as a theoretical data sample in machine learning analyses. We also show an example of the validity of such first-level approximation. Finally, we trace the conclusion of this proceedings in Section 4.

2 Multiple WIMP signatures

In the most general approach, the secondary emission expected by annihilation or decay events of WIMPs in any astrophysical source is given by:

$$\frac{d\Phi_{\rm DM}}{dE}(E, \Delta\Omega, l.o.s.) = P(E) \times J_g(\Delta\Omega, l.o.s). \quad (1)$$

The $P(E)$ and $J_g(\Delta\Omega, l.o.s)$ are the particle physics factor (or source term) and the generalized astrophysical factor, respectively. The specific expression of each of those factors depends on the particular case of interest, as we explain in the following lines. In Fig. 1, we schematically show the WIMP annihilation process (i.e. the P-factor). By each annihilation event, WIMPs produce a couple of SM particle-antiparticle (i.e. leptons, quarks or bosons) which decay and hadronization processes generate fluxes of secondary particles, e.g. gamma rays, neutrinos, matter-antimatter (electron-positron, proton-antiproton, etc...). These fluxes may be observed by detectors on satellites [10, 11] or ground-based Cherenkov telescopes [12, 13, 14, 15]. Each of this particle is considered to be a *messenger* of the information on the nature of the WIMP candidate, i.e. its mass and interaction with the SM particles. In fact, given a WIMP mass and interaction (i.e. a specific DM candidate), the products of the annihilation process are well defined SM particles. SM hadronization and decay processes can produce fluxes of secondary particles, whose spectral shape depends on the first SM channel produced in the WIMP annihilation process. Therefore, the so-called *multi-messenger approach* refers to searching for multiple signatures

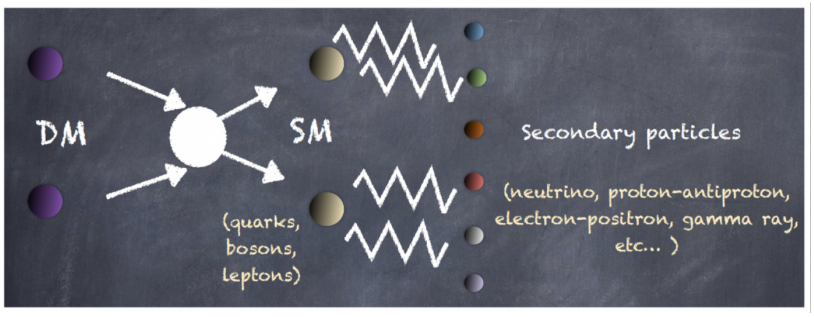

Figure 1: Illustrative schematization of the WIMP annihilation process happening in any astrophysical object dominated by a DM content, e.g. dwarf spheroidal galaxies [18, 19], dwarf irregular galaxies [20, 21], Galactic center [15, 22, 23], galaxy clusters [24]. See text for further details.

of DM candidates in several fluxes of secondary astroparticles. Furthermore, charged particles produced by WIMP annihilation events interact with the magnetic field in our Galaxy or in the emitting source, producing a broad spectra of electromagnetic emission, via e.g. synchrotron emission, inverse Compton, Bremsstrahlung, Coloumb interaction. In this case, the P-factor is indeed the source term of a diffusion equation, which final electromagnetic emission can be detected by several telescope, e.g. with interferometric technique of the Square Kilometer Array (SKA) [16, 17]. In this case, searching for multiple signatures of the same WIMP candidate through several electromagnetic emission is called *multi-wavelength approach*.
Finally, the J_g-factor is defined by the astrophysical target, i.e. the DM dominated astrophysical object where the WIMP annihilation/decay process is happening, e.g. dwarf galaxies [18, 19, 20, 21], the Galactic center [15, 22, 23], galaxy clusters [24]. Indeed, the J_g-factor is the normalization factor, which depends on the amount of DM in the astrophysical target. The calculation of this J_g-factor represents the highest source of uncertainty in indirect searches [25]. Nonetheless, in this proceeding, we focus on the P-factor and related uncertainty.

2.1 Multi-messenger approach

The multi-messenger nature of the indirect searches can be made explicit by rewriting the Eq. 1 as:

$$\frac{d\Phi_{\text{sp-DM}}}{dE} = \frac{\eta_{\text{sp}}}{4\pi} \sum_{a=1}^{2} J^{(a)}_{\text{g-sp}} \cdot \sum_{j}^{\text{SM channels}} \frac{\zeta_j^{(a)}}{\delta m^a_{DM}} \frac{dN^j_{\text{(sp)}}}{dE} \tag{2}$$

This equation describes the expected flux of secondary particles produced by DM annihilation and decay events. The $\eta_{\rm sp}$ parameter is related to both the propagation or deviation of the observed particle[1]; a is related to the DM event: $a = 1$ is for DM decay and $a = 2$ is for DM annihilation. The astrophysical factor $J^{(a)}_{\text{g-sp}}$ is given by the integration along the line of sight of the DM density distribution in the target: in case of DM decay $J^{(1)}_{\text{g-sp}} \propto \rho_{DM}$ and for DM annihilation $J^{(2)}_{\text{g-sp}} \propto \rho^2_{DM}$. The SM channels (quarks, bosons or leptons) are the products of DM decay or annihilation: the branching ratios of production $Br_j = \zeta_j^{(a=2)} / < \sigma v >$ or $Br_j = \zeta_j^{(a=1)} \tau^{-1}_{\rm decay}$ is the probability of annihilation/decay in each SM channel. In the model independent approach for thermal WIMPs, the WIMP candidates annihilate (decay) into one SM channel with 100% of probability ($B_r = 1$), i.e. $\zeta_j^{(a=2)} =< \sigma v >$ ($\zeta_j^{(a=1)} = \tau^{-1}_{\rm decay}$). Instead, in a model dependent approach, the combination of different SM channels and their branching ratios depends on the specific WIMP candidate. Finally, $\frac{dN^j_{\rm (sp)}}{dE}$, is the differential flux of secondary particles expected by each DM annihilation or decay event. It depends on the SM channel and it is generally computed with Monte Carlo events generator software. More details on Eq. 2 can be found in [26], with a particular focus on the Galactic Very Inner Region (VIR) and the multi-TeV WIMP candidate.

2.2 Multi-wavelength approach

In this section we briefly introduce the reader to the connection between multi-messenger and multi-wavelength signals from WIMP annihilation events. During the transport of the secondary cosmic rays in the galactic environment, the deflection of charged particles by the galactic magnetic field would result in the emission of electromagnetic radiation. In the case of ultra-relativistic particles, the emission is produced through synchrotron radiation in a continuous frequency range. Indeed, ultra-relativistic e^+/e^- are responsible for a large number of signatures in the sky, being the synchrotron emission one of the main mechanisms of energy losses. Such an e^+/e^- propagation is dominated by the diffusion equation:

$$-\nabla \cdot [D\,(\mathbf{r}, E)\,\nabla\psi] - \frac{\partial}{\partial E}\,[b(\mathbf{r}, E)\psi] = Q_e(\mathbf{r}, E) \tag{3}$$

where $D\,(\mathbf{r}, E)$ is the diffusion coefficient, $\nabla\psi$ is the number density of charged particles after propagation, $b(\mathbf{r}, E)$ is the energy loss term, and $Q_e(\mathbf{r}, E)$ is the source term. If the primary source of injected electrons is the annihilation of WIMPs, the source term is given by:

[1] E.g. $\eta_\gamma \approx 1$ for a gamma ray, which travels undeflected in the local Universe

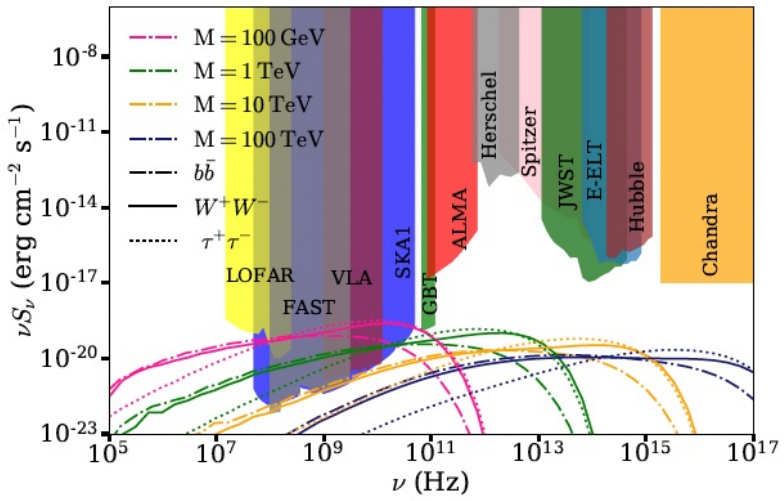

Figure 2: Flux density for a Draco-like dSph in the range of frequencies $10^5 - 10^{17}$ Hz as produced by the Synchrotron emission of secondary e^+e^- for different DM masses and annihilation channels. Colour bands represent the sensitivity regions of several detectors. Targets with a radio signal boost mechanism could improve the competitiveness of these detectors. Figure from [16].

$$Q_e(\mathbf{r}, E) = \frac{1}{2} \langle \sigma v \rangle \left(\frac{\rho_{\rm DM}(\mathbf{r})}{M} \right)^2 \sum_j \beta_j \frac{{\rm d}N_e^j}{{\rm d}E}. \tag{4}$$

The diffusion Eq. 3 is a simplification of the Ginzburg-Syrovatsky transport equation. The latter takes into consideration some other mechanisms such as re-acceleration of cosmic rays (negligible in the case of ultra-relativistic e^+/e^-), spallation of cosmic rays, radioactive decay of nuclei of the interstellar medium as well as eventual interactions with the galactic wind [16, 17]. Indeed, the multi-wavelength approach is also affected by the uncertainty in the description of the galactic and extra-galactic magnetic field. In Fig. 2 [16], we show the multi-wavelength Synchrotron emission produced in the range of frequencies $10^5 - 10^{17}$ Hz by secondary e^+e^- produced by several WIMPs masses and annihilation channels. WIMP candidates at GeV energy scale are suitable to be detected in radio frequencies, yet TeV DM would be better detected at higher frequencies. Even though SKA1 exhibits a competitive sensitivity to measure signatures of WIMPs up to 10 TeV (yellow lines), for heavier TeV WIMPs, the maximum of emission shifts to frequencies higher than the SKA1 range.

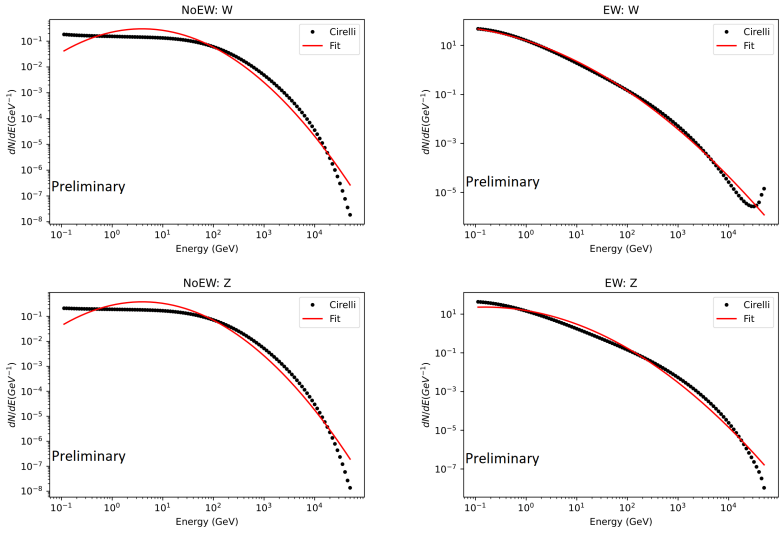

Figure 3: LP fits of the gamma-ray flux simulated with `PYTHIA 8` for a WIMP mass of 50 TeV, annihilating 100% in W^+W^- or ZZ with (EW) or without (NoEW) the electroweak contribution.The values of the parameters can be found in Tab. 1.

3 WIMP signatures and machine learning

In the benchmark data-fitting approach, any detected spectra of both astroparticles or electromagnetic emission is fitted via the differential flux expected by WIMP annihilation events. Indeed, the spectral shape is fixed by the WIMP mass while the amplitude of the signal is a degenerate case of both the astrophysical J-factor and e.g. the annihilation cross section (see Eq. 2). Moreover, an uncertainty on the amplitude is introduced by the multiplicity of secondary particles produced in each annihilation event, which changes with the Monte Carlo event generator software [27]. In [28] a new approach to search for WIMP signatures among a sample of detected but unidentified sources[2] is proposed. The latter is inspired by the data-driven Log Parabola (LP) first fit of any detected source of the Femi-LAT catalogues [29, 30, 31]:

$$\frac{dN}{dE} = N_0 \left(\frac{E}{E_0}\right)^{-\alpha-\beta\cdot\log(E/E_0)} . \tag{5}$$

where N_0 is the gamma-ray flux normalization, E_0 the pivot energy, α the gamma-ray spectral index and β the curvature. Note this parametric form is reduced to a simple power law in the case of $\beta = 0$. From this expression we

[2]Indeed, those sources without any association with known astrophysical sources.

can extract a useful parameter: the peak energy, $E_{\rm peak}$, i.e., the energy at which the energy spectrum $\left(E^2 dN/dE\right)$ is maximum, by performing the consequent derivative, obtaining $E_{\rm peak} = E_0 \cdot e^{\frac{2-\alpha}{2\beta}}$, which represents a signature of different kind of emitting sources.

Parameters	**Z - EW**	**Z - NoEW**	**W - EW**	**W - NoEW**
E_{Peak} (TeV)	0.8 ± 0.3	1.9 ± 0.5	5 ± 2	2.4 ± 0.7
α	0.44 ± 0.04	-0.45 ± 0.05	0.67 ± 0.03	-0.43 ± 0.05
β	0.116 ± 0.004	0.16 ± 0.08	0.078 ± 0.003	0.156 ± 0.005

Table 1: Value of the relevant parameters for the LP fits of the gamma-ray flux simulated with `PYTHIA 8` for a WIMP mass of 50 TeV, annihilating 100% in W^+W^- or ZZ with (EW) or without (NoEW) the electroweak contribution.

In [28, 32] the gamma-ray spectra obtained in the PPPC4DMID [33] for several DM masses and annihilation channels are fitted with a LP, obtaining the same characterization in the parameter space defined by the observational LP modelling. In Tab. 1 and Fig. 3 we show the gamma-ray flux produced by the PPPC4DMID for a WIMP mass of 50 TeV annihilating into W^+W^- (upper panels) and ZZ (lower panels) channels, without the ElectroWeak (EW) corrections (left panels) and by including the EW corrections (right panels). In the left upper panel of Fig. 4 we show the $E_{\rm peak}$, β parameters resulting of the LP fitting of a combination of W^+W^- and ZZ annihilation channels:

$$\frac{dN}{dE} = B_r \left(\frac{dN}{dE}\right)_Z + (1 - B_r) \left(\frac{dN}{dE}\right)_W , \tag{6}$$

where the branching ratio B_r goes from 0 to 1 with a 0.1 step. In the right upper panel of Fig. 4 we show the relative uncertainty ϵ_β/β. In the lower left and right panels we show the same procedure by including the EW contribution. This LP approach allows to search for DM candidates in a broad sample of sources, by applying Machine Learning (ML) algorithms, e.g. an artificial Neural Network (NN) [28]. Within this approach, $E_{\rm peak}$ and β are features for the ML algorithm. In [28] it is also shown that the overall classification accuracy can be improved by including systematic features, which allow to model instrumental systematic uncertainty for the expected DM class. Without entering into the details of that work, in this proceeding we have just introduced the LP data-driven approach for indirect searches of WIMPs by reproducing part of that procedure. Moreover, we also include new preliminary results: the black point in Fig. 4 is indicative of the $E_{\rm peak}$ and β parameters obtained by fitting the Galactic VIR with a LP (see the following section).

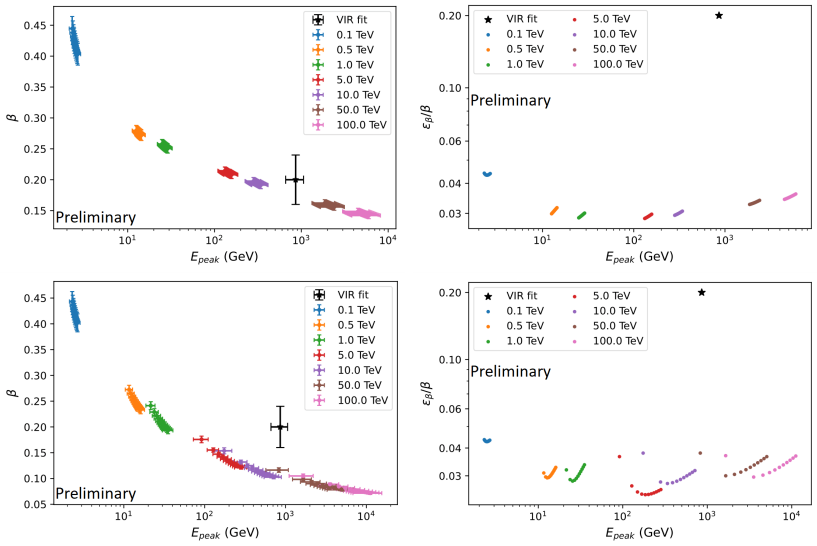

Figure 4: Upper panel: $E_{\rm peak} - \beta$ plot for the LP parametrization of the PPPC4DMID code for several WIMP masses without EW corrections. For each mass in the range from 0.1 to 100 TeV (different colors), different fits have been performed with branching ratios B_r from 0 to 1 with a 0.1 step (as defined in Eq. 6). The relative uncertainty on the β parameter (ϵ_β/β) is showed in the right panel. Lower panels: Same as upper panels, applied to PPPC4DMID code with EW corrections. The black point is the fit of the gamma-ray cut-off detected by HESS in the Galactic VIR (left panel) and its relative error (right panel) (see Sec. 3.1). The relative uncertainty associated with the LP fit of the gamma-ray data dominates on the uncertainty associated with the LP fit of the PPPC4DMID code.

3.1 Example: the Galactic very inner region

In this section we generalize the LP data-drive approach [28, 32] based on Fermi-LAT catalogues to a different gamma-ray detected source, namely, the gamma-ray cut-off detected by HESS at the Galactic VIR [34]. The best fit of these data as DM is obtained by assuming that the total gamma-ray flux is given by a combination of a DM signature more an extra background component of unknown astrophysical origin [22, 23]. The latter is modeled as a power law, while the DM component is given by Eq. 1. The total fit is given by:

$$\frac{d\Phi_{\rm DM}}{dE} = \sum_i^{\rm channels} \frac{\langle\sigma v\rangle_i}{2} \frac{dN_i}{dE} \frac{\Delta\Omega\langle J\rangle_{\Delta\Omega}}{4\pi m_{\rm DM}^2} + B^2 E^{-\gamma} \tag{7}$$

We use the HESS data as an example to cross check the validity of that general approach. In Fig. 5 we show the fit of the HESS data from the Galactic VIR [34] performed with two different Monte Carlo event generator software, namely `PYTHIA 6` and `PYTHIA 8`. In the first case we use the analytical fitting

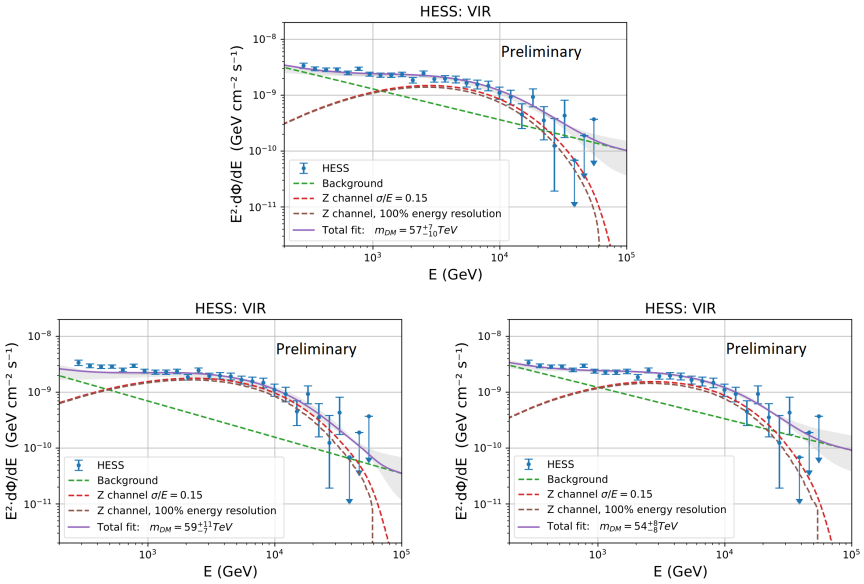

Figure 5: Fit of the gamma-ray flux observed by HESS in the Galactic VIR [34], by assuming a power-law background component and DM signature of WIMPs annihilating in in the Z channel. Upper panel: we adopted the analytic fitting functions of `PYTHIA 6`, [35]), with $\sigma/E = 0.15$ energy resolution. Lower left panel: same as upper panel, but computed with `PYTHIA 8`, including the EW. Lower right panel: Same as left lower panels, but now considering ZZ channel without including the EW corrections.

functions [35], in the second case we use the PPPC4DMID interpolation function [33] (with/out EW corrections). In Tab. 2 we show the parameters of these fits. We performed the fit by taking into account the HESS energy resolution of 15%. By introducing this effect the fitted DM mass is a 14% lower than the value obtained by fitting the data without the instrumental energy resolution. The results are in agreement with [22, 23]. For WIMP masses of $\sim 50 TeV$ annihilating in to the ZZ channel, the uncertainty introduced by using a different version of `PYTHIA` is indeed negligible [27].

Finally, we perform the fit of the HESS Galactic VIR with a LP (Fig. 6). The fitted parameter are shown in Tab. 3. In Fig. 4 we compare the obtained $E_{\rm peak}$ and β with the LP parametrization of the PPPC4DMID code. $E_{\rm peak}$ is compatible with a WIMP candidate of ~ 50 TeV within the uncertainty showed in Tab. 2. The β parameter is compatible with the LP fit of the PPPC4DMID code without the EW correction, in agreement with the best fit value reported in Tab. 2. The relative uncertainty ϵ_β/β of the LP modelling of the PPPC4DMID code is negligible if compared to the relative uncertainty associated to the LP

Parameters	PYTHIA 6	PYTHIA 8 EW	PYHTIA 8 NoEW
m_{DM} (TeV)	57^{+6}_{-10}	59^{+11}_{-7}	54^{+8}_{-8}
$B^2(10^{-8}\ GeVcm^{-2}s^{-1})$	5^{+8}_{-3}	6^{+18}_{-5}	6^{+9}_{-3}
γ	$2.5^{+0.2}_{-0.1}$	$2.6^{+0.2}_{-0.2}$	$2.6^{+0.2}_{-0.1}$
$\langle J\rangle_{\Delta\Omega}$ $(10^{28}\ GeV^2\ cm^{-5})$	4^{+1}_{-1}	5^{+1}_{-1}	4^{+1}_{-1}
$\langle J\rangle_{\Delta\Omega}/J_{EVANS}$ $(\times 10^3)$	$1.4^{+0.3}_{-0.4}$	$2.1^{+0.4}_{-0.5}$	$1.6^{+0.3}_{-0.4}$
χ^2 / ddof	1.33	2.52	1.23
$\Delta\Omega$ (sr)	1.16×10^{-5}		

Table 2: Fitted parameters of the Galactic VIR ($\Delta\Omega$ is the solid angle of the region) as a combination of a WIMP signature and a power-law background (Eq. 7) within 1σ confidence level. We consider the ZZ annihilation channel. The secondary flux of gamma-ray has been simulated with both PYTHIA 6 and PYTHIA 8, with/without the EW effect. We also show the $\chi^2/ddof$ of each fit.

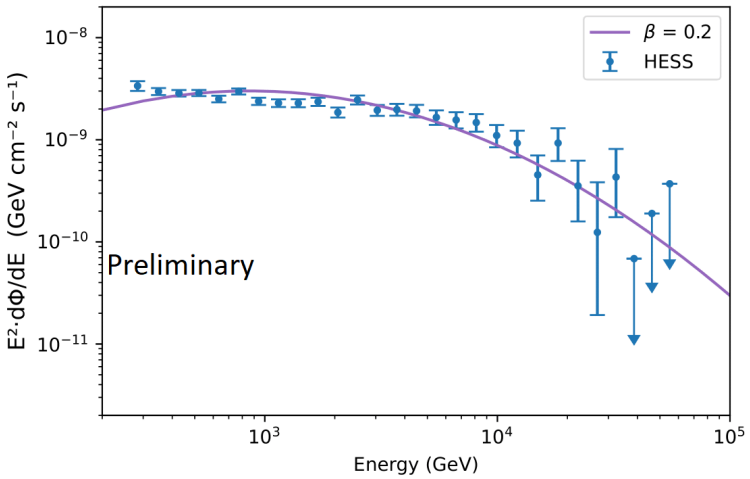

Figure 6: Fit GC with LP, the parameters can be found in Tab. 3.

E_{Peak} (TeV)	α	β	$\chi^2/ddof$
0.9 ± 0.2	2.1 ± 0.1	0.20 ± 0.04	3.03

Table 3: Fitted parameters of the HESS data of the Galactic VIR with the LP.

fit of the VIR gamma-ray spectra .

4 Conclusions

In this proceedings we reviewed both the benchmark approach to indirect detection of WIMP candidate and the Log Parabola (LP) data-driven approach for Machine Learning (ML) application. The multi-messenger and multi-wavelength detection of any WIMP signature would result in a competitive claim of the indirect detection of DM. The first term refers to the study of multiple fluxes of secondary particles, which could be emitted contemporaneously from a same DM candidate. In the second case, the same concept is extended to the study of any electromagnetic emission, produced by the interaction of the secondary flux of charged particles with a magnetic field. All that multiple signatures of WIMP candidates are predicted with Monte Carlo event generator software. Although the use of Monte Carlo software can introduce some uncertainty in the predicted flux of secondary particles, in the case of WIMPs annihilating into ZZ channel, the expected gamma-ray flux can be predicted with high precision. In Fig. 5 and Tab. 3 we show the result of the fit of the gamma-ray cut-off detected by HESS at the Galactic Very Inner Region (VIR) by using the gamma-ray flux simulated by `PYTHIA 6` or `PYTHIA 8` with/out electroweak corrections. All these results are in agreement within the uncertainty.
Moreover, we reviewed the LP data-driven framework developed for the application of ML algorithms to indirect searches for DM. The latter approach focuses on the LP fitting of the expected fluxes of secondary particles. Thus, bringing the theoretical expectation on the experimental parameter space, we can improve the possibility to disentangle prospective WIMP candidates in a vast sample of unidentified sources. In Fig.s 4, 6 and Tab. 3 we show as this approach has a first order validity, and the prospective DM candidate found out with ML algorithms need to be undergo to further analyses.

5 Acknowledgements

The work of VG and JZP was supported by the grants PID2021-125331NB-I00 and CEX2020-001007-S, both funded by MCIN/AEI/10.13039/501100011033 and by "ERDF A way of making Europe". VG's contribution to this work has been supported by *Juan de la Cierva-Incorporación* IJC2019-040315-I grants. JZP's contribution to this work has been supported by *FPI Severo Ochoa* PRE2021-099137 grant.

References

[1] Leszek Roszkowski, Enrico Maria Sessolo, and Sebastian Trojanowski. WIMP dark matter candidates and searches—current status and future prospects. *Rept. Prog. Phys.*, 81(6):066201, 2018.

[2] Anne M Green and Bradley J Kavanagh. Primordial black holes as a dark matter candidate. *Journal of Physics G: Nuclear and Particle Physics*, 48(4):043001, feb 2021.

[3] P. J. E. Peebles, D. N. Schramm, E. L. Turner, and R. G. Kron. The case for the relativistic hot Big Bang cosmology. , 352(6338):769–776, August 1991.

[4] Marc Schumann. Direct Detection of WIMP Dark Matter: Concepts and Status. *J. Phys. G*, 46(10):103003, 2019.

[5] Antonio Boveia and Caterina Doglioni. Dark Matter Searches at Colliders. *Ann. Rev. Nucl. Part. Sci.*, 68:429–459, 2018.

[6] J. A. R. Cembranos, A. Dobado, and Antonio Lopez Maroto. Brane world dark matter. *Phys. Rev. Lett.*, 90:241301, 2003.

[7] Lawrence J. Hall, Karsten Jedamzik, John March-Russell, and Stephen M. West. Freeze-In Production of FIMP Dark Matter. *JHEP*, 03:080, 2010.

[8] Jonathan L. Feng, Arvind Rajaraman, and Fumihiro Takayama. Superweakly interacting massive particles. *Phys. Rev. Lett.*, 91:011302, 2003.

[9] Jennifer M. Gaskins. A review of indirect searches for particle dark matter. *Contemp. Phys.*, 57(4):496–525, 2016.

[10] E. Charles et al. Sensitivity Projections for Dark Matter Searches with the Fermi Large Area Telescope. *Phys. Rept.*, 636:1–46, 2016.

[11] Francesca Calore, Marco Cirelli, Laurent Derome, Yoann Genolini, David Maurin, Pierre Salati, and Pasquale Dario Serpico. AMS-02 antiprotons and dark matter: Trimmed hints and robust bounds. *SciPost Phys.*, 12(5):163, 2022.

[12] Tolga Yapici and Andrew J. Smith. Dark Matter Searches with HAWC. *PoS*, ICRC2017:891, 2018.

[13] Michele Doro. A review of the past and present MAGIC dark matter search program and a glimpse at the future. In *25th European Cosmic Ray Symposium*, 1 2017.

[14] H. Abdalla et al. Search for Dark Matter Annihilation Signals in the H.E.S.S. Inner Galaxy Survey. *Phys. Rev. Lett.*, 129(11):111101, 2022.

[15] A. Acharyya et al. Sensitivity of the Cherenkov Telescope Array to a dark matter signal from the Galactic centre. *JCAP*, 01:057, 2021.

[16] J. A. R. Cembranos, Á De La Cruz-Dombriz, V. Gammaldi, and M. Méndez-Isla. SKA-Phase 1 sensitivity to synchrotron radio emission from multi-TeV Dark Matter candidates. *Phys. Dark Univ.*, 27:100448, 2020.

[17] Sergio Colafrancesco, Marco Regis, Paolo Marchegiani, Geoff Beck, Rainer Beck, Hannes Zechlin, Andrei Lobanov, and Dieter Horns. Probing the nature of Dark Matter with the SKA. *PoS*, AASKA14:100, 2015.

[18] M. Ackermann et al. Searching for Dark Matter Annihilation from Milky Way Dwarf Spheroidal Galaxies with Six Years of Fermi Large Area Telescope Data. *Phys. Rev. Lett.*, 115(23):231301, 2015.

[19] Tjark Miener, Daniel Nieto, Viviana Gammaldi, Daniel Kerszberg, and Javier Rico. Constraining branon dark matter from observations of the Segue 1 dwarf spheroidal galaxy with the MAGIC telescopes. *JCAP*, 05(05):005, 2022.

[20] V. Gammaldi, E. Karukes, and P. Salucci. Theoretical predictions for dark matter detection in dwarf irregular galaxies with gamma rays. *Phys. Rev. D*, 98(8):083008, 2018.

[21] Viviana Gammaldi, Judit Pérez-Romero, Javier Coronado-Blázquez, Mattia Di Mauro, Ekaterina Karukes, Miguel Angel Sánchez-Conde, and Paolo Salucci. Dark Matter search in dwarf irregular galaxies with the Fermi Large Area Telescope. *PoS*, ICRC2021:509, 2021.

[22] J. A. R. Cembranos, V. Gammaldi, and A. L. Maroto. Possible dark matter origin of the gamma ray emission from the galactic center observed by HESS. *Phys. Rev. D*, 86:103506, 2012.

[23] J. A. R. Cembranos, V. Gammaldi, and A. L. Maroto. Spectral Study of the HESS J1745-290 Gamma-Ray Source as Dark Matter Signal. *JCAP*, 04:051, 2013.

[24] Judit Pérez-Romero. Sensitivity of CTA to gamma-ray emission from the Perseus galaxy cluster. *PoS*, ICRC2021:546, 2021.

[25] N. W. Evans, J. L. Sanders, and A. Geringer-Sameth. Simple J-Factors and D-Factors for Indirect Dark Matter Detection. *Phys. Rev. D*, 93(10):103512, 2016.

[26] Viviana Gammaldi. Multimessenger Multi-TeV Dark Matter. *Front. Astron. Space Sci.*, 6:19, 2019.

[27] J. A. R. Cembranos, A. de la Cruz-Dombriz, V. Gammaldi, R. A. Lineros, and A. L. Maroto. Reliability of Monte Carlo event generators for gamma ray dark matter searches. *JHEP*, 09:077, 2013.

[28] V. Gammaldi, B. Zaldívar, M. A. Sánchez-Conde, and J. Coronado-Blázquez. A search for dark matter among Fermi-LAT unidentified sources with systematic features in Machine Learning. 7 2022.

[29] S. Abdollahi et al. *Fermi* Large Area Telescope Fourth Source Catalog. *Astrophys. J. Suppl.*, 247(1):33, 2020.

[30] The Fermi-LAT Collaboration. Fermi Large Area Telescope Third Source Catalog. *APJS*, 2015.

[31] The Fermi-LAT Collaboration. 3FHL: The Third Catalog of Hard Fermi-LAT Sources. *APJS*, 232:18, October 2017.

[32] Javier Coronado-Blázquez, Miguel A. Sánchez-Conde, Mattia Di Mauro, Alejandra Aguirre-Santaella, Ioana Ciucă, Alberto Domínguez, Daisuke Kawata, and Néstor Mirabal. Spectral and spatial analysis of the dark matter subhalo candidates among Fermi Large Area Telescope unidentified sources. *JCAP*, 11:045, 2019.

[33] Marco Cirelli, Gennaro Corcella, Andi Hektor, Gert Hutsi, Mario Kadastik, Paolo Panci, Martti Raidal, Filippo Sala, and Alessandro Strumia. PPPC 4 DM ID: A Poor Particle Physicist Cookbook for Dark Matter Indirect Detection. *JCAP*, 03:051, 2011. [Erratum: JCAP 10, E01 (2012)].

[34] F. Aharonian et al. Spectrum and variability of the Galactic center VHE γ-ray source HESS J1745-290. , 503(3):817–825, September 2009.

[35] J. A. R. Cembranos, A. de la Cruz-Dombriz, A. Dobado, R. Lineros, and A. L. Maroto. Fitting formulae for photon spectra from WIMP annihilation. *J. Phys. Conf. Ser.*, 314:012063, 2011.